Aalto University
School of Engineering

Xiaomi Yang

Characterizing car to two-wheeler residual crashes in China: Application of the automatic emergency braking system in virtual simulation

Author Xiaomi Yang

Title of thesis Characterizing car to two-wheeler residual crashes in China: Application of the automatic emergency braking system in virtual simulation

Master programme Mechanical Engineering   **Code** ENG25

Thesis supervisor Kari Tammi

Thesis advisor(s) Jonas Bärgman

Date 24.06.2019   **Number of pages** 35   **Language** English

Abstract

The fast development of vehicles not only benefits people's life, but also threatens people's health in the road traffic. The Automatic Emergency Braking (AEB) system is one effective active safety system in saving lives on the road . This study proposed one AEB algorithm and it was implemented to car-to-two-wheeler crashes to evaluate the performance of the AEB, with the aim to analyze the characteristics of the remaining crashes. The algorithm was based on comfort braking and steering limits of car drivers and two-wheeler drivers, and the algorithm simulation was com-posed of the future path prediction of both vehicles, the braking maneuver and the steering maneuver of car drivers and two-wheeler drivers. The simulation of the future path prediction was used to check whether the car and the two-wheeler was on the collision course and the braking and steering maneuvers were to assess the collision avoidance ability of both drivers. The proposed algorithm was triggered only when the collision danger was detected and both drivers could not avoid the collision by steering or braking on their own. The reference algorithm, which utilized the vehicle braking limitation and did not involve the collision avoidance ability of the drivers, was only applied to compare the effectiveness in collision avoidance. Both AEB algorithms were applied to the pre-crash-matrix (PCM) of the China Shanghai United Road Traffic Scientific Research Center (SHUFO) crash data. It was found that the proposed algorithm was triggered later than the reference algorithm in about 50% of cases. In these cases, the drivers may feel it unnecessary to activate the AEB when the reference algorithm was triggered, as they were still able to avoid the collision by their own action or by the action of the collision partner. To evaluate the in-jury mitigation, one available motorcyclist injury model from previous research was used in the study. The injury mitigation was studied based on the three levels of injury: MAIS2+F, MAIS3+F and fatal injury. The results indicated that the effectiveness in injury mitigation for fatal injury is around 60% and for MAIS2+F and MAIS3+F, around 50% after the proposed AEB implementation. The proposed algorithm is applicable to all types of car-to-two-wheeler scenarios. The crash data was classified into nine types of scenarios and the simulation results showed that the effectiveness of the proposed AEB algorithm in collision avoidance varied across scenarios. Straight moving car scenarios have a higher proportion of residual crashes compared to the turning car scenarios. This may be due to the differences in the cars traveling speed.

Keywords AEB algorithm, collision avoidance, powered two-wheeler, SHUFO PCM, comfort limits of drivers

Preface

Zhengzhou 24.6.2019

Xiaomi Yang

Contents

Notations

Abbreviation

ABS	Anti-lock Braking System
AEB	Automatic Emergency Braking
AIS	Abbreviated Injury Scale
BTN	Brake Threat Number
CA	Collision avoidance
CIDAS	China In-Depth Accident Study
C-NCAP	China New Car Assessment Program
Euro NCAP	European New Car Assessment Programme
GIDAS	German In-Depth Accident Study
ITTC	Inverse TTC
IVT	Inter-Vehicle-Time
MAIS2+F	Injury level equals to AIS2, and higher and fatal
MAIS3+F	Injury level equals to AIS3, and higher and fatal
PCM	Pre-Crash Matrix
PTWs	Powered Two-wheelers
SHUFO	China Shanghai United Road Traffic Scientific Research Center
STN	Steering Threat Number
TTC	Time-to-Collision
VRUs	Vulnerable road users

Roman upper case letters

C_f	Front cornering stiffness
C_r	Rear cornering stiffness
L_w	Wheelbase
M	Mass of vehicle
P	Injury risk
R	Radius

Roman lower case letters

a^{lat}	Lateral acceleration
c	Curvature
j^{lat}	Lateral acceleration jerk
k_f	Normalized front cornering compliance
k_r	Normalized rear cornering compliance
v	Speed
v_r	Relative speed

Greek letters

α_f	Front tire slip angle
α_r	Rear tire slip angle
β	Sideslip angle
δ	Steering angle
θ	Steering wheel angle
$\dot{\theta}$	Steering wheel angle rate
ϕ	Course angle
ψ	Heading angle

1 Introduction

1.1 Background and literature review

The number of vehicles in use has steadily increased with the development of transportation (World Health Organization, 2018). From 2005 to 2015, the vehicle use in the Europe increased from 321 million to 388 million, while in China and the United States, vehicle use increased from 32 million to 163 million, and 238 million to 264 million respectively (OICA, 2018). Powered Two-wheelers (PTWs), which are defined as two-wheeler powered by a combustion engine or rechargeable batteries, including motorcycles, scooters and e-bikes (Genève & Bastiaensen, 2014), are one popular vehicle class as they take less space, use less fuel, are cheaper, and allow more flexible use than cars (Bartolomeos et al., 2017).

The popularity of PTWs varies across countries. Low- and middle-income countries make up the majority users of PTWs (World Health Organization, 2018). The use of e-bikes, especially, has grown rapidly in many countries in Asia and Europe. The number of e-bikes in China, for example, has increased from approximately 40,000 in 1998 to about 170 million in 2014 (Bartolomeos et al., 2017). Figure 1.1 shows one scene of PTWs at one traffic intersection in China.

Figure 1.1   The traffic intersection in Zhengzhou, China

The development of cars and PTWs has created easy and convenient mobility options. However, cars and PTWs threaten people's health at the same time. 1.35 million people die every year because of the road traffic accidents (World Health Organization, 2018). In fact, the road traffic injury has become one major cause of death for people across all age groups (World Health Organization, 2018).

Vulnerable road users (VRUs) constitute more than half of all road traffic deaths, and powered two-wheeler drivers are one type of the vulnerable road users (World Health Organization, 2018). According to the World Health Organization, in 2015, PTWs accounted for 14% of traffic fatalities while passengers of 4-wheeled cars and light vehicles took up

17% in the United States (World Health Organization, 2018). One year later, still in the United States, with an increase of 5.1%, 5,286 motorcyclists were killed. In fact, in 2016, the fatalities of motorcyclists per vehicle miles was 28 times higher than passenger car driver fatalities. What's more, 14% of all traffic fatalities and 17% of all occupant (driver and passenger) fatalities occurred in motorcycle accidents in 2016 (NHTSA, 2018). Also, in New South Wales, with only 3.7% of all registered motor vehicles being PTWs, they, in 2012, accounted for 15% of the fatalities and 10% of the injuries in traffic accidents (New South Wales Government, 2012). Similarly, in Iceland, PTWs, which constituted less than 2% of all licensed vehicles in 2008, accounted for 12% of the road accident fatalities and almost 5% of all fatalities (Road Safety Authority, 2014). In the European Union, approximately 26,100 people were killed in PTWs road accidents and accounted for 18% of all traffic fatalities (European Commission, 2015). In China, 26,200 deaths and 157,500 injuries were caused because of PTWs in 2005 (Li et al., 2008).

These fatality and injury numbers should have risen people's awareness regarding the safety of PTWs. However, even though PTWs have a lot of safety concerns, the current safety systems for PTWs is not widely available in some countries. For example, in China and Brazil, ABS (Anti-lock Braking System) is only required for vehicles with greater than 250cc and 300cc engine respectively. This suggests smaller motorcycles are excluded from ABS requirement (World Health Organization, 2018), therefore, the safety of motorcycles is still a worrying situation.

To protect people's health from the safety threats of traffic accidents, there is a need to improve vehicle safety. Safety systems, including airbags and strong body structures, have been playing an important role in saving people's lives, and belong to passive safety features (O'Neill, 2009). Besides these traditional passive safety systems, new possibilities of safety systems arise with the development of modern sensors and computer technologies (Coelingh, Lind, Birk, & Wetterberg, 2006). Automakers help drivers in avoiding crashes before they happen by actively assisting the driver in the driving task (Coelingh, Eidehall, & Bengtsson, 2010). Such systems are called active safety systems. Collision avoidance (CA) system is one important part of active safety technology, including functionality to alert the driver of imminent danger, or even automatic braking (Brännström, Coelingh, & Sjöerg, 2009).

Automatic Emergency Braking (AEB) system is defined as a vehicle system that automatically applies braking by the vehicle to potentially avoid the collision when the collision danger is detected (Euro NCAP, 2018). AEB systems have shown great potential in avoiding or mitigating traffic accidents (Sander, 2018), and safety assessment programmes also attach more importance to AEB. The European New Car Assessment Programme (Euro NCAP) which provides star rating regrading vehicle safety to consumers, added the introduction of a new protocol of assessment of AEB system into different categories of the adult occupant protection and the safety assist in 2014. In the China New Car Assessment Program(C-NCAP), AEB tests have been added from 2018. The AEB tests include pedestrian autonomous emergency braking system tests (AEB VRU_Ped) and tests of autonomous emergency braking systems (AEB CCR) in a rear collision (China Automotive Technology and Research Center, 2018).

Most AEB systems are composed of three parts: sensors, a processing unit and triggering actuators (Jiang, He, Liu, & Zhu, 2014). As a lot of attention has been given to the collision

avoidance solutions, threat-assessment methods have been improved over the years. A widely used time domain threat assessment method is Time-to-Collision (TTC). TTC values are used as thresholds to determine warning or automatic braking maneuvers (Horst et al., 1993). TTC-based algorithms have different types of computation and the most widely used is to simply divide distance between the two vehicles by the relative speed (Dahl, de Campos, Olsson, & Fredriksson, 2018).

Some metrics similar to TTC have also been proposed, including Inverse TTC (ITTC) and Inter-Vehicle-Time (IVT) (Jansson, 2005; Kiefer et al., 2004; Noh & Han, 2014). In addition, acceleration based threat assessment methods, which involve the vehicle braking level, have also been developed and studied by many researchers (Brännström, Coelingh, & Sjöberg, 2010, 2014). The Brake Threat Number (BTN) and the Steering Threat Number (STN) are metrics used to evaluate when to activate the AEB system (Brännström, Sjöberg, & Coelingh, 2008). BTN is the required longitudinal acceleration divided by the maximum vehicle longitudinal acceleration and STN is the required lateral acceleration divided by the maximum vehicle lateral acceleration. Therefore, when BTN and STN are larger than 1, it means the required acceleration is larger than the maximum acceleration and the crash cannot be avoided. When the values of BTN or STN are equal to 1, it suggests the required acceleration has reached the maximum acceleration provided by the vehicle and the AEB system should not wait or an accident could happen.

Traditional acceleration based threat assessment methods adopt a constant acceleration model for the host and target vehicles (Coelingh, Jakobsson, Lind, & Lindman, 2007). This algorithm has many assumptions regarding vehicle dynamics, such as, the heading angle of the host vehicle keeps constant and the acceleration can jump to any value without a time interval. Other researchers have investigated a new method where the host vehicle instead is assumed to keep a constant curvature with a constant jerk (time-derivative of acceleration) (Dahl et al., 2018). However, traditional algorithms can mainly be implemented in rear-end collision situations (Brännström et al., 2010). Actually, most available AEB systems on the market today are only designed for rear-end collisions, even though in principle, AEB can be implemented in all types of collisions (Coelingh et al., 2010).

If the AEB system only brakes with a constant jerk and the maximum acceleration limitation, when the AEB activates the car driver and the opponent driver may still have the chance to avoid crash by braking or steering on their own (Brännström et al., 2010). Therefore, it may cause unnecessary activation of the AEB system. In places where the traffic situation is less organized, for example in China, road users get used to small spaces and they would usually adjust speed in the intersection (Tageldin, Sayed, & Wang, 2016). This supports the idea that only considering the system (vehicle) braking limitation, but not the driving abilities of the driver, is not practical. With all these factors considered, taking the avoidance ability of drivers into account is a natural and important step to improve AEB algorithms.

Some researchers have studied the AEB algorithm based on comfortable thresholds of the car driver and the opponent driver (Brännström et al., 2010, 2014; Sander, 2018). This is also the approach used in this thesis. The comfortable thresholds are considered for both braking and steering. The braking thresholds include the maximum braking acceleration and the maximum braking acceleration jerk (time-derivative for the longitudinal acceleration). The steering thresholds include the maximum steering wheel angle, the maximum steering wheel angle rate, the maximum lateral acceleration and the maximum lateral jerk (time-

derivative for the lateral acceleration). The comfortable thresholds for the car driver braking and steering are taken from other previous researches (Brännström et al., 2010). However, very few references have been found regarding the comfortable thresholds of two-wheeler drivers, especially for the braking limit. The steering thresholds for two-wheeler drivers are chosen according to the available simulation results of other researchers (Costa et al., 2019).

Most of available research about the AEB system are based on European data, such as the German In-Depth Accident Study (GIDAS) dataset (Jeppsson, Östling, & Lubbe, 2018). Data generated by pre-crash scenario simulation is contained in so called Pre-Crash Matrix (PCM) data. The PCM data describes the pre-crash-sequences of accidents in detail (Schubert, Erbsmehl, & Hannawald, 2013). Characteristics of the traffic and crashes can vary a lot across countries. To study crash characteristics in China, usually two real world accident databases are used, including the China In-Depth Accident Study (CIDAS) and China Shanghai United Road Traffic Scientific Research Center (SHUFO) (Ding, Bohman, Zhang, Li, & Zhao, 2016; Sui, Zhou, & Lubbe, n.d.). The data used in this simulation is SHUFO database. The crashes collected in SHUFO are from the Shanghai Jiading district where passenger cars are involved in a crash with an injury or high economy loss (Ding et al., 2016). Autoliv restructured SHUFO data in the same way as GIDAS PCM, called SHUFO PCM hereafter.

Injuries can be classified in different ways. One way is to divide injury levels according to the Abbreviated Injury Scale (AIS), which was developed by the Association for the Advancement of Automotive Medicine to define the severity of injuries throughout the body with respect to probability of mortality (Gennarelli & Wodzin, 2006). Many researchers have used the Maximum Abbreviated Injury Scale (MAIS) to evaluate the injury results (Ding, Rizzi, Strandroth, Sander, & Lubbe, 2019). For example, MAIS2+F level includes injuries with maximum AIS of level 2 and higher and fatalities.

Research shows that the impact speed is one influential factor for motorcyclist injuries (Hurt Jr, Thom, & Ouellet, 1981). One example of an injury risk model in literature used relative impact speed for MAIS2+F, MAIS3+F and Fatal injury levels (Ding et al., 2019). By implementing AEB, some accidents can be avoided and some can be mitigated, leading to the reduction of the impact speed. The injury of accidents avoided by the AEB algorithm is lowered to zero, while the injury of the remaining crashes is calculated according to the injury risk curve for all three injury levels (Sander, 2018).

1.2 Aim and objective

This project has two aims. The first aim is to design an AEB algorithm based on the comfort limits of drivers, targeting avoidance and mitigation of car-to-two-wheeler crashes in China. The second aim is to characterize the car to two-wheeler crashes that remain after the AEB algorithm has been applied to Chinese crash kinematics data.

1.3 Scope

The data used in this study is from the Chinese SHUFO crash database, including only crashes between cars and two-wheelers. The objective of the work is to evaluate the AEB algorithm performance and describe the remaining crash characteristics. The AEB system was designed for cars and the AEB intervention only involves the braking based on the car's maximum braking ability, while the algorithm considers possible actions by the driver and two-wheeler drivers (within their comfort zones) in activating the AEB. The maneuvers of

two-wheeler (and car) drivers are thus considered in the algorithm design, but in this study the two-wheeler is assumed not to have an AEB system.

2 Methods

This chapter presents the data used in this study, simulation details and the injury model used. The data was introduced in the subsection and it was classified into nine scenarios for further result analysis. The simulation framework was carried out based on previous work (Rosén, 2013). The proposed algorithm and the reference algorithm were presented in this chapter. The motorcyclist injury model was adopted for further injury risk analysis (Ding et al., 2019).

2.1 Data

The SHUFO database is composed of the reconstructed crash data in Shanghai, China (Ding et al., 2016). In SHUFO database, the accidents of passenger cars with injury or high economy loss were recorded (Ding et al., 2016). This section presents the SHUFO PCM data, characteristics of the data and classification of the scenarios in the database.

2.1.1 SHUFO PCM data

The reconstructed cases are available in the SHUFO database, but the SHUFO PCM is not directly available. Instead, it was created by researchers from Autoliv by following the same structure of the GIDAS PCM. The PCM data contains data generated by pre-crash scenario simulation and it describes the pre-crash-sequences of accident in detail (Schubert et al., 2013). The SHUFO PCM contains vehicle dynamics information including velocity, acceleration and heading angle, and other vehicle parameters, such as, weight, length, width, wheelbase. All these variables are used in this study to design and evaluate the AEB algorithm.

2.1.2 Dataset characteristics

A total of 71 crashes from the SHUFO data was used in this study. Different from the GIDAS with the pre-crash data of 5s, the time series of the SHUFO PCM data vary from 0s to 6s. The distribution of pre-crash data length is shown in Figure 2.1. It shows that for 16 cases the duration of the available PCM crash data is less than 2s. The frequency of data is 100Hz and corresponding the time step is 0.01s.
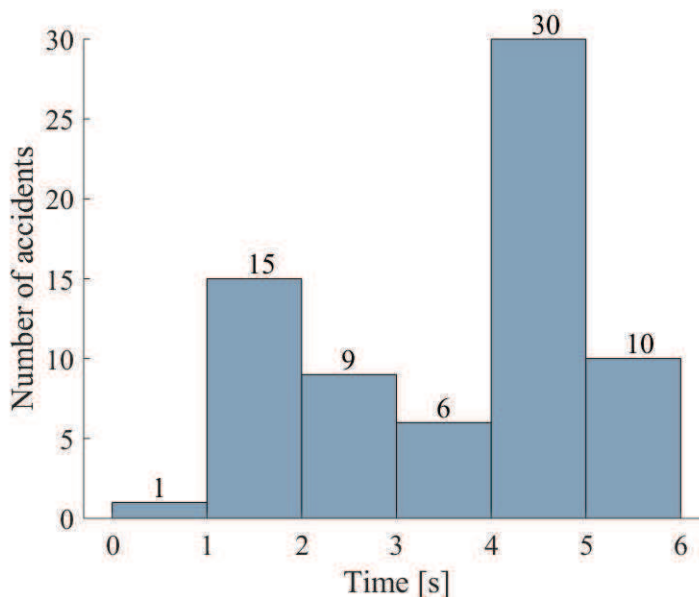

Figure 2.1   Distribution of the length of the dataset

2.1.3 Scenario classification

The SHUFO data contains different kinds of scenarios. It is necessary to cluster scenarios before designing the AEB algorithm. The scenario was first roughly classified by the course direction of the car and the two-wheeler. The course directions classifications are : straight going, left turning and right turning. During the classification, more than one situation was found in 'straight going' type scenario. Therefore, the 'straight going' scenario was further separated into: 'Straight crossing', 'Straight front to front' and 'Straight two-wheeler still' three types. In three cases, the velocity of two-wheeler is zero and car is straight going. These cases were joined to the scenario type 'two-wheeler still'. The remaining 'straight going' cases were divided according to the heading directions of the car and the two-wheeler. Cases with less than $15°$ heading angle difference were grouped into 'front to front' type, while cases whose heading angle difference was between $45°$ and $135°$ were categorized as the 'straight crossing' type. The heading angle illustration of both types are shown in Figure 2.2.
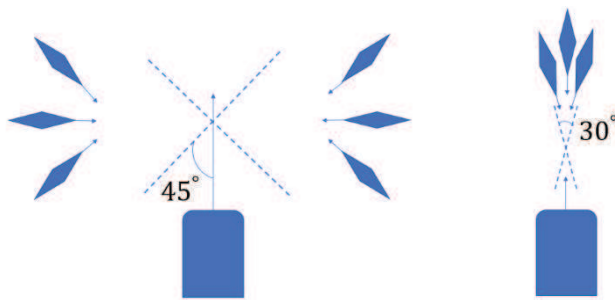
Figure 2.2   Illustration of 'straight crossing' and 'front to front' scenarios. Left is the 'straight crossing' type and the right is the 'front to front' one.

Based on the definitions of classification above, all 71 cases were grouped into a specific scenario type. The case classification results are shown in Table 2.1 and the numbers are the case numbers.

Table 2.1   Scenario classification for all accident case numbers.

Car \ Two-wheeler	Straight	Left turning	Right turning
Straight crossing	2, 4, 5, 9, 10, 11, 14, 15, 16, 18, 70, 69, 68, 66,65, 62, 61,55, 54, 53, 52, 50, 45, 44, 40,39,38, 37, 36, 34, 26,23	1, 7, 8, 17, 19, 20, 22, 56, 49, 47, 42, 41,35, 33, 31, 30, 29, 28	6, 12, 57
Straight front to front	3, 67		
Straight two-wheeler still	21,63, 71		
Left turning	60,51, 48, 46, 43, 27, 25, 24		64
Right turning	13,59, 58	32	

The distribution of all accident scenarios from the dataset can be seen in Figure 2.3. It suggests that the straight crossing type is the most common scenario, accounting for 45% of all crashes. The second largest group is the 'car straight and two-wheeler turning left' scenario with 25%. It is followed by the 'car turning left and two-wheeler going straight' scenario with 11%. The cases for both the car and the two-wheeler turning are very few.
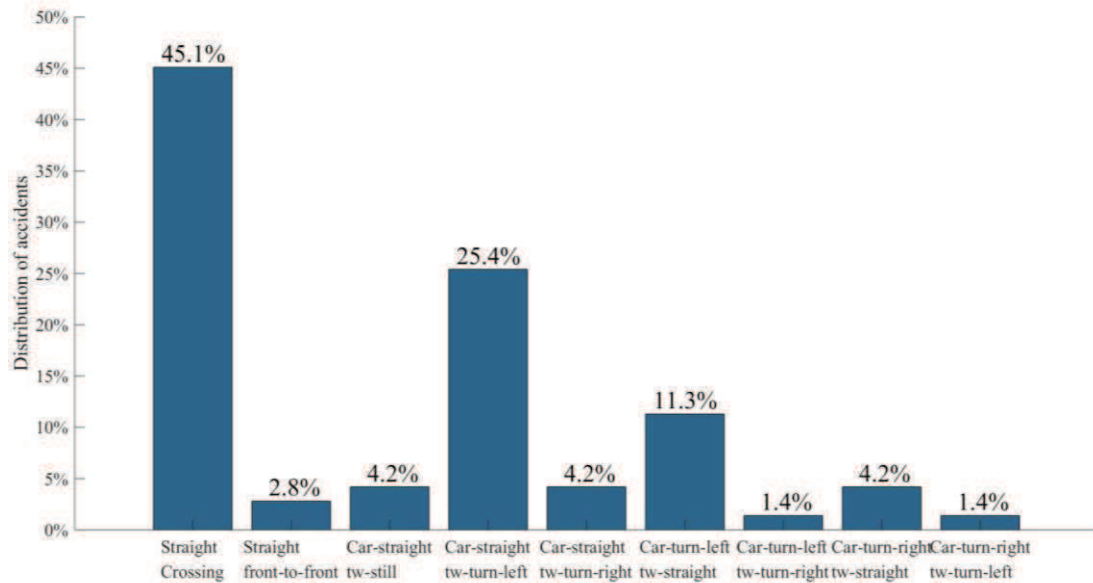
Figure 2.3   Distribution of accident scenarios.

2.2 Simulation framework

The simulation of the AEB algorithm was based on the framework of the Matlab implementation applied to the PCM dataset and the framework was adopted from other researcher (Rosén, 2013). The framework starts by importing data, followed by a sensor model and an algorithm simulation. The framework ends with the algorithm evaluation. The first three parts, 'Import data', 'Case selection' and 'Sensor model' belong to the old framework (which was provided at the start of the work) and the remaining parts are related to the proposed algorithm is a contribution from this thesis. The flowchart of the framework is shown in Figure 2.4.
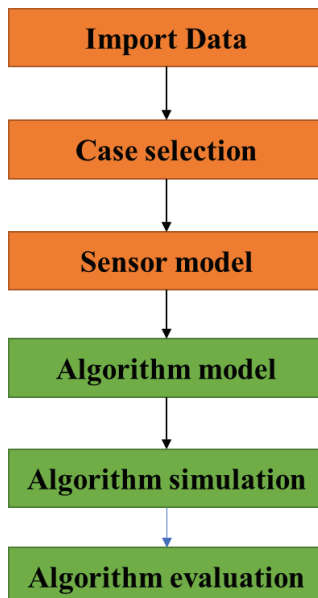
Figure 2.4   Flow chart of the simulation framework.

The imported data was structured in the PCM with categories of global data, participant data, dynamic, library special road marks and library standard objects. The case selection

was to pick up all the car to the two-wheeler crashes by case type. The sensor model computed distance and angles between the two-wheeler and the sensor mounted in the car. The AEB algorithm simulation did not start computing until two-wheeler was visible in the range of the sensor. After the two-wheeler was within the field of view of the sensor and within range, the next step for the algorithm was to judge whether the car was going to collide with the two-wheeler based on the future path prediction. If the danger of a collision was predicted, simulations of braking and steering maneuvers would have started, otherwise the simulation would have kept computing the prediction path. The trigger time was based on the maneuvers of both drivers. Once the trigger time was decided, automatic emergency braking would be applied to the crash data and the performance of AEB system can be evaluated by the remaining crash results.

2.3 Proposed AEB algorithm

The AEB algorithm presented in this work considered the possible braking and steering maneuvers of both the car driver and the two-wheeler driver to avoid collision. This section describes the algorithm logic, future path prediction, the braking maneuver and the steering maneuver – the four main parts of the proposed AEB algorithm.

2.3.1 Algorithm logic

The AEB system is activated only if the following conditions are satisfied:
1) *The two-wheeler is visible and within the sensor field of view and range*
2) *The car is predicted on the collision course with the two-wheeler*
3) *The braking maneuver of the car driver cannot avoid the collision*
4) *The steering maneuver of the car driver cannot avoid the collision*
5) *The braking maneuver of the two-wheeler driver cannot avoid the collision*
6) *The steering maneuver of the two-wheeler driver cannot avoid the collision*

The flow chart shown in Figure 2.5 explains the principle of the proposed AEB algorithm.
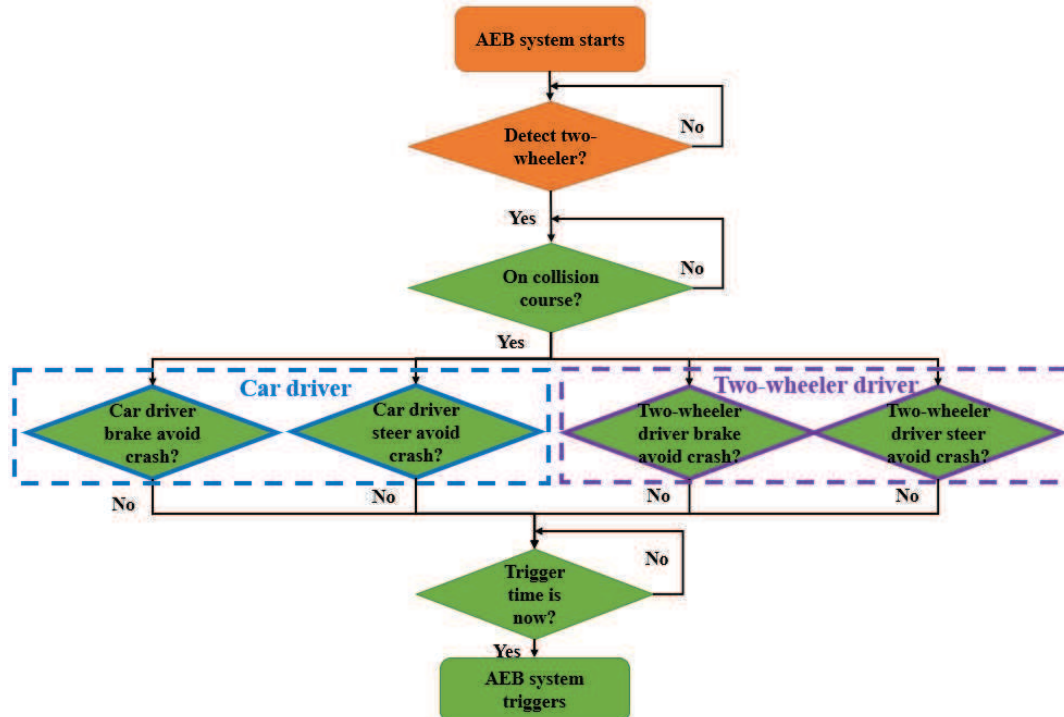

Figure 2.5   The flow chart of the AEB algorithm model. Orange parts are from another researcher (Rosén, 2013) and green parts are from the author.

The geometry of two-wheeler is simplified as a rhombus and the car as a rectangle without front two corners according to PCM data standard. The visibility is calculated for each corner of the two-wheeler. The further path prediction is based on the current and past kinematics data of both the car and the two-wheeler. Braking and steering maneuvers are computed based on the comfort limits of the car driver and the two-wheeler driver. The AEB system triggers when both drivers cannot avoid collision by either steering or braking. Therefore, it is advantageous to analyze four important time points when the driver perform avoidance maneuvers but are not able to avoid the collision. The time points are described as the latest escape time point for car drivers or two-wheeler drivers to steer or brake. They are outlined as:

- T_{Brake}^{Car} : the latest escape time point for the car driver to brake.
- T_{Steer}^{Car} : the latest escape time point for the car driver to steer.
- T_{Brake}^{Tw} : the latest escape time point for the two-wheeler driver to brake.
- T_{Steer}^{Tw} : the latest escape time point for the two-wheeler driver to steer.

2.3.2 Future path prediction

After the AEB system has detected the two-wheeler by using the sensor model, the next step is to check whether the car is going to collide with the two-wheeler. The prediction of the future path is to compute the positions of the car and the two-wheeler in the future, which can be calculated by the velocity and the driving direction predicted in the future. As shown in equation (2.1), in an small time interval, the changes of the position Δx and Δy in Cartesian coordinate system are computed by the velocity and the course angle:

$$\Delta x = v\cos\phi$$
$$\Delta y = v\sin\phi$$

(2.1)

The velocity and the course angle in the future are dependent on the current and past kinematics data of both the car and the two-wheeler. The predictions of the velocity and the course angle are based on some assumptions. One assumption for the driving direction is that if the car or the two-wheeler is on a straight path, then it would keep going straight in the future, otherwise, it would keep turning with the same turning radius. To judge whether the current driving path is straight or turning, the yaw rate is taken into consideration. At each time point, for the past 0.2s, if the car or the two-wheeler has a yaw rate more than $0.025\,rad/s$, the car or the two-wheeler is assumed to be on a turning path. Otherwise, the car or the two-wheeler is assumed to be on a straight path, with the same driving direction in the predicted path. One more assumption is that the car and the two-wheeler move with the current velocity and without longitudinal acceleration in the future path. Based on these assumptions, the future turning paths for the car and two-wheeler are computed.

For future turning path estimation, the radius is assumed to be constant. As the curvature c is the inverse of the radius, shown in equation (2.2), the curvature is also constant.

$$c = \frac{1}{R}$$

(2.2)

The course angle ϕ is essential for position calculation. The course angle is

$$\phi(t) = \int w(t)dt = \int \frac{v_0}{R(t)} dt = \int c(t)v_0 dt \qquad (2.3)$$

The yaw rate $\dot{\phi}(t)$ is the derivation of the yaw angle $\phi(t)$, and it is shown in the equation (2.4). As the curvature and the velocity are assumed to be constant, the yaw rate is also constant.

$$\dot{\phi}(t) = c(t)v_0 \qquad (2.4)$$

Thus, the car or the two-wheeler keeps turning with the constant yaw rate for the turning path. To check whether the car and the two-wheeler collide or not, both the car and the two-wheeler are computed in the future path and the predicted position are checked at each time step. If the predicted position has any intersection between the two vehicles, then they are predicted to collide, otherwise they are not on collision course for that time step. For each time step, the simulation predicts 5s in the future, or until a collision is detected. Predicted TTC time is the time duration from the predicting time point until the predicted collision time and it was used to analyze the AEB implementation results.

Figure 2.6 shows one example of a predicted future path. It presents the predicted path when the car is at the trigger time point. The car is predicted to be on the straight going path while the two-wheeler on the turning path. It shows that the future path prediction is relatively precis for this event. The shapes of the car and the two-wheeler for the prediction path are 1.5 times larger as the original shapes for threat calculation in the algorithm to make the AEB system more sensitive to possible road dangers and compensate the error in prediction.
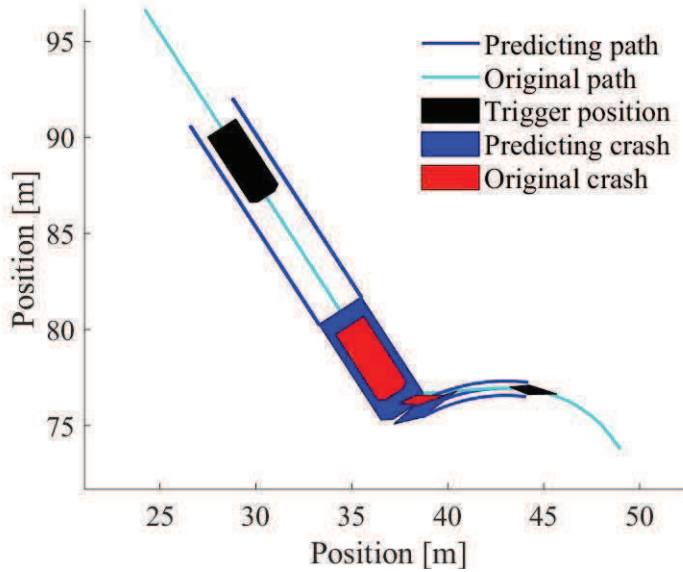
Figure 2.6   One example of the future path prediction. The car is presented with a rectangle shape and two-wheeler with a rhombus. The light blue line is the original path and red shapes are the original collision positions, while the dark blue line is the predicted path and dark blue shapes are the predicted collision positions.

2.3.3 Braking maneuver

By applying the comfort braking limits of car drivers and two-wheeler drivers, the latest escape time points for braking maneuver ($T_{brake}^{driver}, T_{brake}^{tw}$) can be obtained. Comfort braking

limits for the car drivers were studied from other literature (Bärgman, Smith, & Werneke, 2015; Brännström et al., 2010, 2014), while for the two-wheeler drivers, braking levels were chosen between car drivers and cyclists braking abilities (Uittenbogaard, Op den Camp, & van Montfort, 2016).

2.3.3.1 Braking principle

Potential braking maneuvers were characterized by the maximum acceleration a_r and the maximum acceleration jerk j_r. The related input braking parameters are shown in Figure 2.7.

Figure 2.7   Parameters illustration of braking maneuver

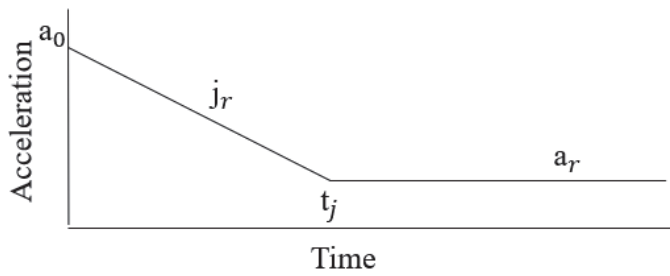It is assumed that the car or the two-wheeler stops turning when the car driver or two-wheeler driver brakes, and the opponent keeps travelling on the predicted path (see, 2.3.2, Future path prediction). It means that the vehicle, whose driver takes the braking maneuver, is traveling straight with the course direction while the opponent is not influenced by the braking. In this case, the ground-fixed Cartesian coordinate system is adopted. For a small time interval, the changes of the positions are the integration of the velocity, and the changes of the velocity is the integration of the acceleration. The value of the acceleration has a turning point at time t_j. Before t_j, the acceleration changes linearly with a constant jerk j_r, and after t_j, the acceleration reaches the maximum value and keeps the same value until vehicle stops. The calculation of t_j is shown in equation (2.5).

$$t_j = \frac{a_r - a_0}{j_r} \qquad \textbf{(2.5)}$$

Comfortable braking limits of car drivers have been studied or used in some literatures, and the values are between 3m/s² to 5m/s² (Bärgman et al., 2015; Brännström et al., 2014; Sander, 2017). However, to the knowledge of author, comfortable braking limits of powered two-wheeler are not available in current literature. In this study we assume that the braking ability of a (Bärgman et al., 2015; Uittenbogaard et al., 2016) PTW should be between a cyclist and a car driver, for which information is available . The ranges of the comfortable braking limits used in this study are shown in Table 2.2. For the simulation results shown in Chapter 3, the input comfortable braking acceleration for car driver and two-wheeler driver is -5 m/s^2 and jerk is -5 m/s^3.

Table 2.2 Comfortable braking limits of drivers

Parameters	Driver	Two-wheeler
$a_{min}(m/s^2)$	-7~-3	-7~-3
$j_{min}(m/s^3)$	-7~-3	-7~-3

2.3.3.2 Braking case example

A braking case example of the two-wheeler is shown in Figure 2.8. It shows the path of the car and the two-wheeler after the two-wheeler starts braking.
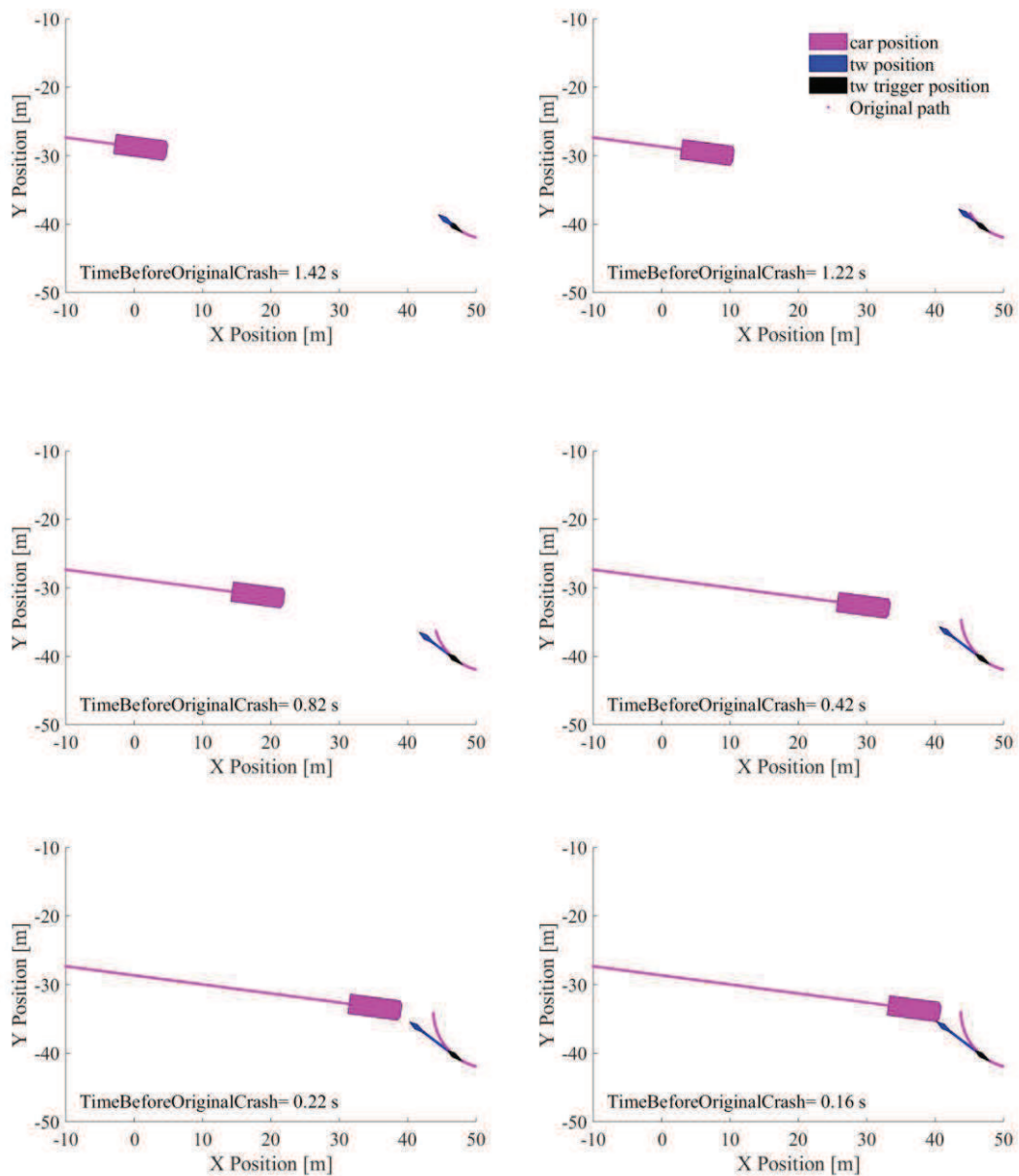

Figure 2.8   Illustration of braking maneuver of the two-wheeler driver

2.3.4 Steering maneuver

For the steering maneuver, a linear bicycle model (Abe & Manning, 2009; Brännström et al., 2010) is used for both the car and the two-wheeler. Besides, the input steering parameters were obtained from literature as comfortable steering limits of both drivers (Brännström et al., 2010, 2014; Costa et al., 2019).

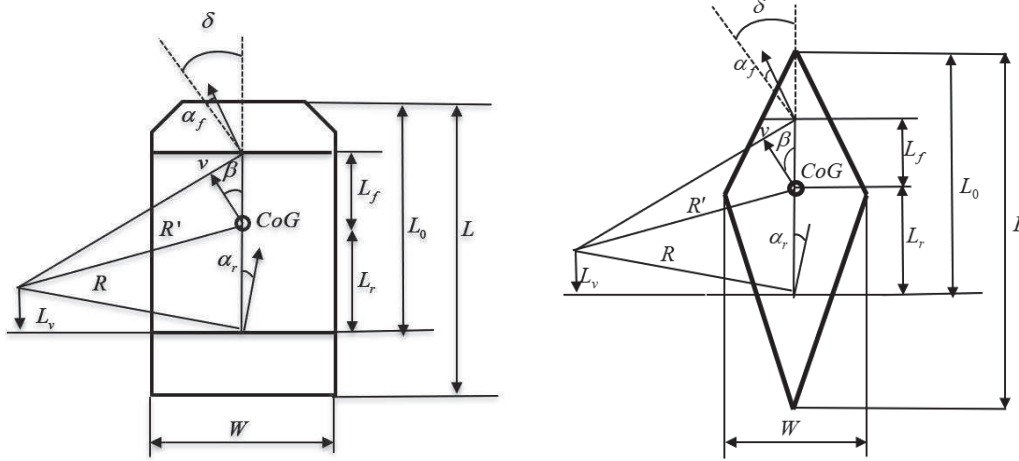### 2.3.4.1 Linear bicycle model

Figure 2.9   Linear bicycle model illustrations for the car and the two-wheeler. The car is presented with a rectangle without front two corners in the left and the two-wheeler with a rhombus in the right. CoG is the center of gravity.

The steering angle is calculated as equation (2.**6**) according to the linear bicycle dynamics. L_w is the wheelbase. c is the curvature.

$$\delta = L_w c + \alpha_f - \alpha_r \qquad (2.6)$$

The rear tire slip angle and the front tire slip angle are calculated as equation (2.7) and (2.8) . M is the mass of vehicle, and v is the velocity. C_r and C_f are the rear and front cornering stiffness (in newtons per radian) while k_r and k_f are the normalized rear and front cornering compliance respectively.

$$\alpha_r = \frac{ML_f}{L_w C_r}\frac{v^2}{R} = \frac{k_r v^2}{R} = k_r c v^2 \qquad (2.7)$$

$$\alpha_f = \frac{ML_r}{L_w C_f}\frac{v^2}{R} = \frac{k_f v^2}{R} = k_f c v^2 \qquad (2.8)$$

By solving the equations (2.6), (2.7) and (2.8), the relation between the steering angle and the curvature is shown in equation (2.9), where $k = k_f - k_r$.

$$\delta = c(L_w + kv^2) = ck_\delta \qquad (2.9)$$

According to the relation between the steering wheel angle θ and the steering angle δ shown in the equation (2.10), the curvature can be calculated through the steering wheel

angle θ as equation (2.11), where $c_0 = \dfrac{\theta_0}{nk_\delta}$ and $c_1 = \dfrac{\dot{\theta}_c}{nk_\delta}$. It means that θ_0 and $\dot{\theta}_c$ are two restriction conditions of the curvature.

$$\delta(t) = \frac{\theta(t)}{n} \tag{2.10}$$

$$c(t) = \frac{\delta(t)}{k_\delta} = \frac{\theta_0 + \dot{\theta}\tilde{t}_\theta}{nk_\delta} = c_0 + c_1\tilde{t}_\theta \tag{2.11}$$

The relationship between lateral acceleration and the curvature is

$$a^{lat}(t) = \frac{v_0^2}{R(t)} = c(t)v_0^2 \tag{2.12}$$

Thus, the curvature can be computed based on the lateral acceleration a_{lat}, shown in equation(2.13), where $c_0 = \dfrac{a_0^{lat}}{v_0^2}$ and $c_1 = \dfrac{j_0^{lat}}{v_0^2}$. It means that a_0^{lat} and j_0^{lat} are another two restriction conditions of the curvature.

$$c(t) = \frac{a^{lat}(t)}{v_0^2} = \frac{a_0^{lat} + j_0^{lat}\tilde{t}_a}{v_0^2} = c_0 + c_1\tilde{t}_a \tag{2.13}$$

The sideslip angle calculated at CoG is

$$\beta = cL_r - \alpha_r \tag{2.14}$$

As shown in the equation (2.15), the longitudinal distance of the turning center is

$$L_v = R'\sin\alpha_r \approx R\alpha_r = k_r v^2 \tag{2.15}$$

Thus, the sideslip angle at CoG is

$$\beta = c(L_r - L_v) \tag{2.16}$$

The relationship among the heading angle ψ, the course angle ϕ and the sideslip angle β is

$$\phi(t) = \psi(t) + \beta(t) \tag{2.17}$$

For a small time interval, changes of positions (x, y) in ground-fixed Cartesian coordinate system are shown as Δx and Δy in equation (2.18) and (2.19).

$$\Delta x = v_0 \cos(\phi(t))\Delta t \tag{2.18}$$

$$\Delta y = v_0 \sin(\phi(t))\Delta t \tag{2.19}$$

The course angle is

$$\phi(t) = \int w(t)dt = \int \frac{v_0}{R(t)} dt = \int c(t)v_0 dt \tag{2.20}$$

2.3.4.2 Steering principle

The steering wheel angle, which linearly changes with a constant steering wheel angle rate, is the input for the steering maneuver. The lateral acceleration and the lateral acceleration jerk are utilized as restriction limits for the maximum curvature. In normal driving conditions, drivers usually steer with a constant steering angle rate and then with a constant steering angle (Godthelp, 1986). In the steering simulation, the steering wheel angle changes

linearly with a constant steering wheel angle rate until it reaches the maximum value. This type of steering is referred as the 'J-steering type'. Figure 2.10 shows the parameterization.
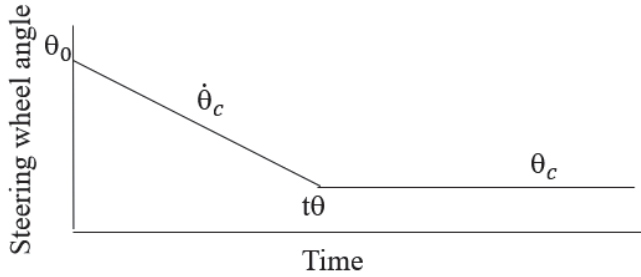

Figure 2.10 Parameters illustration of the steering maneuver

Comfort limits of the car driver and the two-wheeler driver are taken into consideration when steering maneuvers are designed. The simulation input values of comfort steering maneuvers of car drivers and two-wheeler drivers are taken from related literatures and are shown in Table 2.3.

Table 2.3 Comfortable steering limits of car and two-wheeler drivers (Brännström et al., 2010, 2014; Costa et al., 2019)

Parameters	Driver	Two-wheeler
$a_{max}^{lat}\ (m/s^2)$	5	5
$j_{max}^{lat}\ (m/s^3)$	5	5
$\theta_c\ (°)$	720	3
$\dot{\theta}_c\ (°/s)$	400	3
Steering ratio	15	1

The car or two-wheeler velocity is assumed to be constant when the steering maneuver happens. Considering practical driving situations, the changes of the heading angle during steering is limited to $\frac{\pi}{2}$. In the simulation, once the car or the two-wheeler has turned $\frac{\pi}{2}$, it is assumed to continue straight. In addition, both sides, turning left and right are considered as potential steering maneuvers. T_{steer}^{driver} and T_{steer}^{tw} are chosen from the later time for left and right steering.

2.3.4.3 Steering case example

To understand the steering maneuver better, a steering case example for a two-wheeler is shown in Figure 2.11. It shows the trajectory of a two-wheeler for both turning left and right over time.
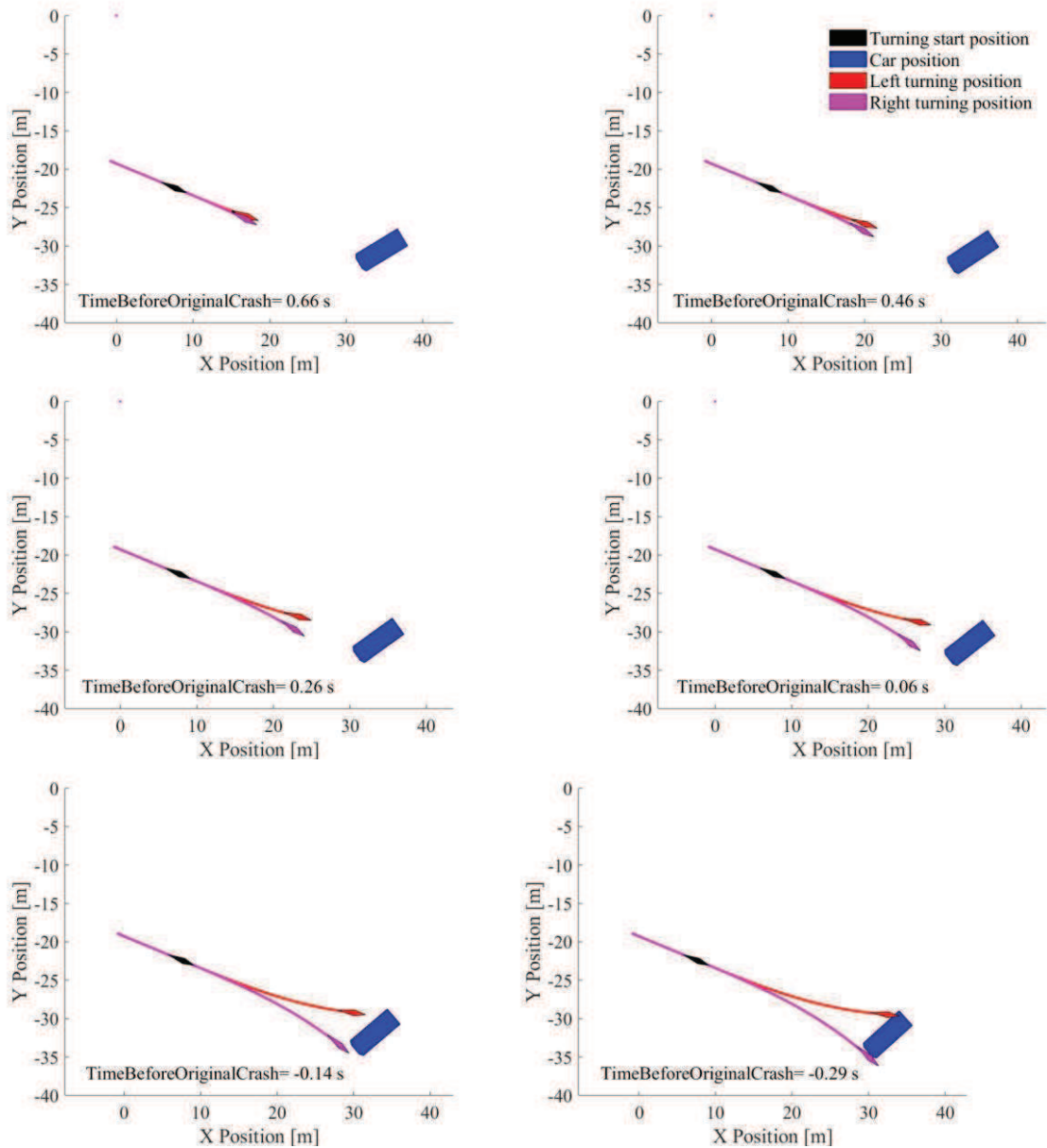
Figure 2.11   Illustration of the steering maneuver of a two-wheeler driver

2.3.4.4 Reference algorithm

To evaluate the performance of the proposed AEB algorithm after the implementation to SHUFO crash data, a reference algorithm was also presented. Different from the proposed AEB algorithm, which is mainly based on the comfort limits of drivers, the reference algorithm utilizes the maximum braking limit of the vehicle. The maximum braking limit of the vehicle includes the maximum braking acceleration and maximum braking acceleration jerk. While the maximum braking acceleration was taken from the original data by adopting the road friction coefficient, and maximum braking jerk was taken from other literature (Brännström et al., 2008). As this reference algorithm is only based on the system parameters, driver behaviors are not taken into consideration.

The reference algorithm is not one traditional acceleration-based algorithm and it is not restricted by other conditions other than braking limit of the vehicle. It is a concept relevant to traditional acceleration-based algorithm. Some traditional acceleration-based algorithms adopt a constant acceleration model for two vehicles and assume the host vehicle does not change heading angle (Coelingh et al., 2007). The same simulation framework was used for the reference algorithm.

2.4 Injury risk

The Abbreviated Injury Scale (Gennarelli & Wodzin, 2006) has been utilized to evaluate injury risks by many researchers. It was also used in this study. When the injury risks was analyzed, slight injury levels were excluded and the injury levels taken into consideration are MAIS2+F, MAIS3+F and fatal injury.

2.4.1 Injury risk curve

To evaluate the injury risk for the remaining crashes after the AEB implementation, one available injury risk model (Ding et al., 2019) is adopted. This model was developed based on the GIDAS motorcycle crashes and it was used to evaluate the injury risks of the SHUFO PCM car to two-wheeler crashes. $P(x)$ is the injury risk and it is calculated based on the equation (2.21), where $t = \beta_0 + \beta_1 x_1 + ... + \beta_n x_n$.

$$P(x) = \frac{1}{1 + e^{-t}} \qquad\qquad (2.21)$$

The influential coefficients are shown in Table 2.4 and the input parameters are applicable to the situations when the motorcycle driver impacts the passenger car on the side and the motorcycle is stable before crash.

Table 2.4   Parameters of Injury risk level model (Ding et al., 2019)

Parameters	MAIS2+F	MAIS3+F	Fatal
Intercept	−2.256	−3.952	−7.175
Relative speed	0.033	0.025	0.035
Impact on driver	0.047	0.529	0.71

The motorcyclist risk curve is shown in Figure 2.12.
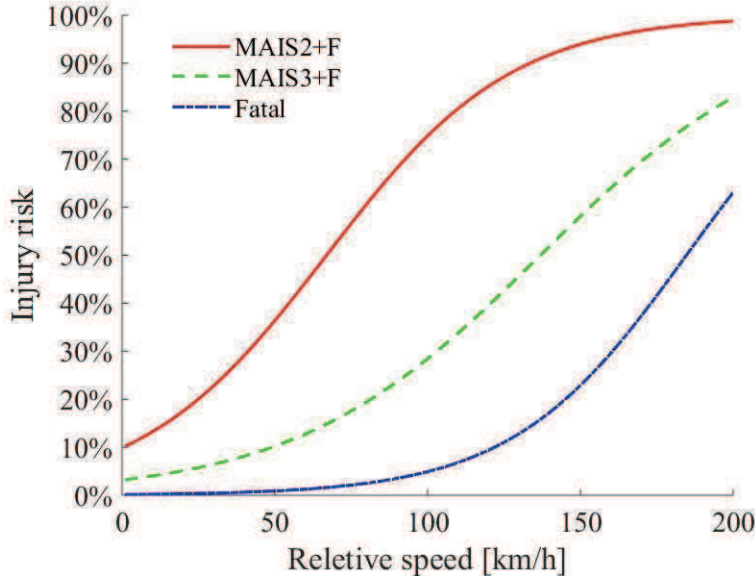
Figure 2.12   Motorcyclist injury risk curve (Ding et al., 2019).

The risk model involves the relative speed as the influential factor. To calculate the relative crash speed for a two-wheeler, the law of cosine is adopted as shown in equation (2.22) and (2.23).

$$\gamma = \phi_{tw} - \phi_{car} \qquad (2.22)$$

$$v_r = \sqrt{v_{car}^2 + v_{tw}^2 - 2v_{car}v_{tw}\cos(\gamma)} \qquad (2.23)$$

The relation among the relative speed v_r, the car speed v_{car} and the two-wheeler speed v_{tw} is shown in Figure 2.13.

Figure 2.13   Car and two-wheeler crash relative speed

2.4.2 Injury reduction effectiveness

The system effectiveness calculation was based on the equation (2.24) (Jeppsson et al., 2018). I is the original crash injury risk and I' is the new injury risk for the remaining crashes after AEB implementation.

$$E = \frac{N - N'}{N} * 100\% = (1 - \frac{N'}{N}) * 100\% \qquad (2.24)$$

3 Results

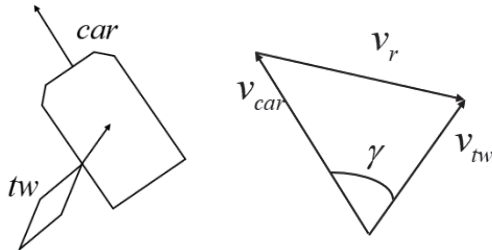This chapter describes the results after the AEB algorithm is applied to the SHUFO crash dataset. The AEB algorithm effectiveness and remaining crash characteristics are both outlined. Moreover, the injury risk reduction for the AEB for motorcyclist is presented. This chapter is first followed by the introduction of the overall performance of the AEB algorithm compared with the reference AEB algorithm, which includes: AEB trigger time, TTC and brake duration, AEB effectiveness and overall Injury. The next section focuses on the residual crashes, including: residual crashes distribution, trigger speed scatter plots, impact speed changes and remaining crash injuries.

3.1 AEB algorithm simulation results

3.1.1 AEB trigger time

The proposed algorithm is based on the comfort limits of car drivers and two-wheeler drivers (see, 2.3, Proposed AEB algorithm), while the reference algorithm is based on the braking limit of the vehicle (see, 2.3.4.4, Reference algorithm), without taking into account that the drivers may feel that the AEB intervention was not warranted, as manual comfortable avoidance was still possible (see, 2.3.4.4, Reference algorithm, for details) . The performance of the proposed AEB algorithm was compared with the reference AEB algorithm. Figure 3.1 shows the trigger time difference. The trigger time for the proposed algorithm is the last point when a driver cannot avoid a crash, while the trigger time for the reference algorithm is the last point when the collision can be avoided by the vehicle braking limitation. The trigger time difference is the trigger time based on the proposed AEB algorithm minus that of the reference AEB algorithm. The Figure 3.1shows that for 23% of the cases, the trigger time based on the proposed algorithm is less than that of the reference AEB algorithm and for about 52% of the cases, the trigger time based on the proposed algorithm is greater than that of the reference AEB algorithm. This plot indicates that both car and two-wheeler drivers have the potential to avoid accidents on their own, even after the trigger time based on the reference AEB algorithm.
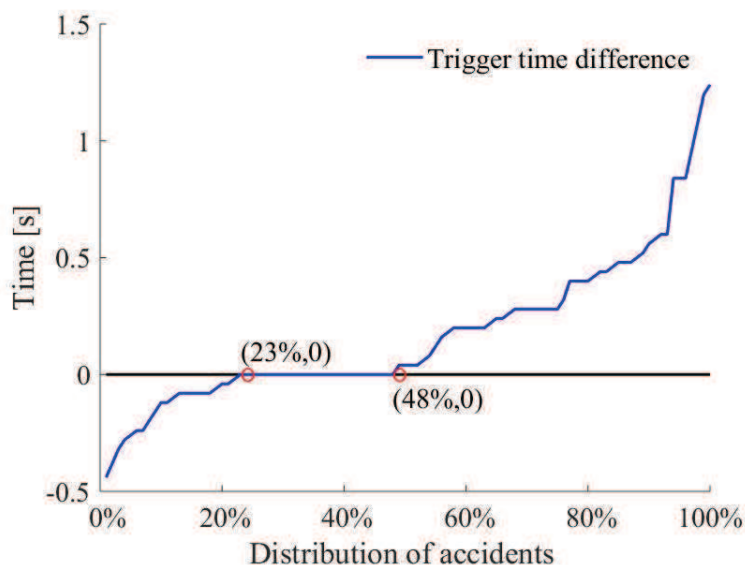

Figure 3.1   Comparison of the trigger times. The blue line represents the trigger time difference based on trigger time of the proposed algorithm minus the trigger time of the reference AEB algorithm.

The TTC time comparison is shown in Figure 3.2. It shows that the TTC at the proposed AEB algorithm trigger point is smaller than TTC at the reference AEB algorithm trigger point. It means that the proposed algorithm triggers when the situation is more severe.
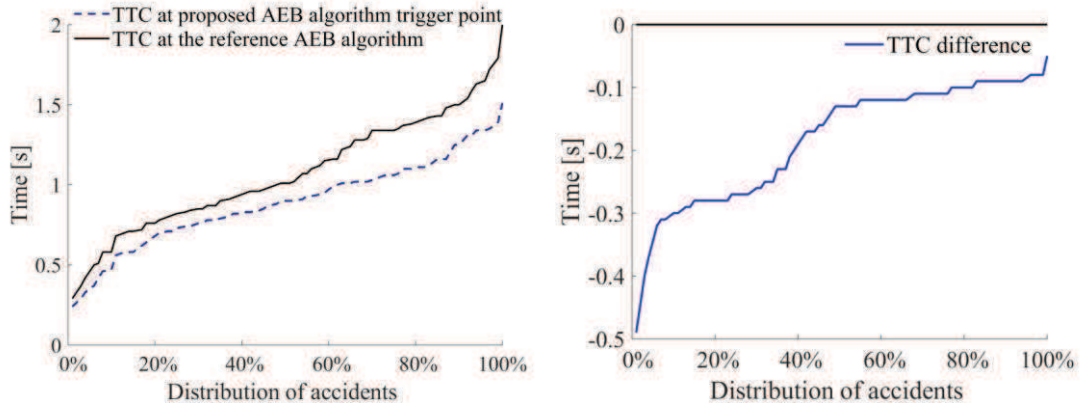

Figure 3.2   TTC time comparison between the proposed AEB algorithm and the reference AEB algorithm at trigger time. The difference of TTC is shown in the right figure. The black line is the zero-reference line.

In addition to the TTC, the brake duration is also one important time indicator, which starts from the activation of the AEB and ends when the new collision takes place, or the car stops. As shown in Figure 3.3, the brake duration of the proposed AEB algorithm is shorter than that of the reference AEB algorithm.
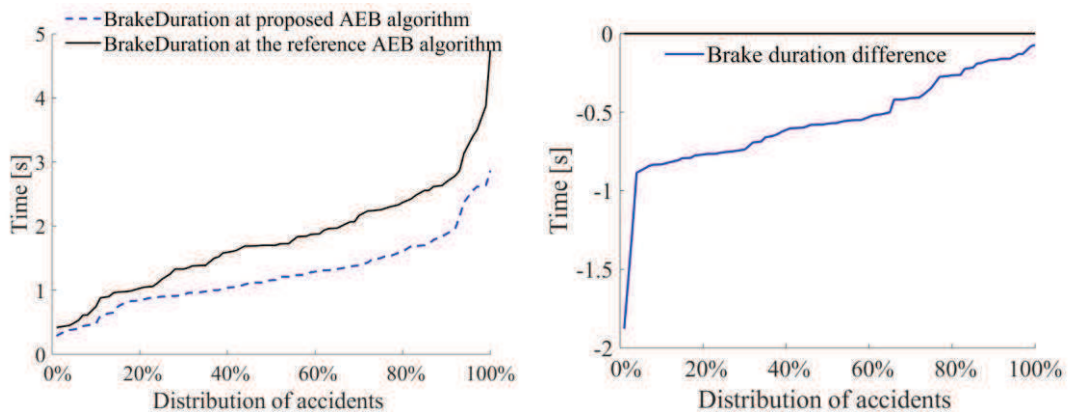
Figure 3.3   Brake duration comparison between the proposed AEB algorithm and the reference AEB algorithm at trigger time. The difference of brake duration is shown in the figure on the right. The black line is the zero-reference line.

3.1.2 AEB performance

When it comes to the performance of the AEB, it is evaluated by the number of avoided crashes. The effectiveness of the reference AEB algorithm, with respect to crash avoidance, is approximately 71%, which is more than double the effectiveness of the proposed algorithm as shown in the Table 3.1. Note, however, that the proposed algorithm considers system acceptance and minimizes nuisance AEB interventions, while the reference system does not.

Table 3.1   The AEB performance for the reference AEB algorithm and the proposed algorithm

Algorithm type	Avoided cases by AEB	Unavoided cases by AEB
Reference AEB algorithm	71.83%	28.17%
Proposed algorithm	35.21%	64.79%

3.1.3 Overall injury effectiveness

The overall injury effectiveness shows that the fatal injury level has been reduced by approximately 57%, while the MAIS2+F and the MAIS3+F injury risks are both reduced by approximately 50%.

Table 3.2   Mean effectiveness of injuries regarding all accidents

Injury level	MAIS2+F	MAIS3+F	Fatal
Mean effectiveness	49.63%	50.73%	57.22%

3.2 Crash analysis

3.2.1 Remaining crashes distribution

Figure 3.4 shows the distribution of all crash scenarios as well as the distribution of the remaining crashes after AEB implementation. For the remaining crashes, the distribution plot shows that the 'Straight Crossing' scenario has the largest proportion of the remaining crashes, followed by the 'Car straight and two-wheeler turn left' scenario. This result matches the total accidents distribution where these two scenarios occur most frequently. However, the third biggest scenario, the 'Car turn left and two-wheeler straight' scenario, with 4% remaining crash rate, accounts for 11% of the total accidents amount. It suggests that the AEB algorithm has a better effectiveness of 'Car turning left, two-wheeler going straight' scenario type.
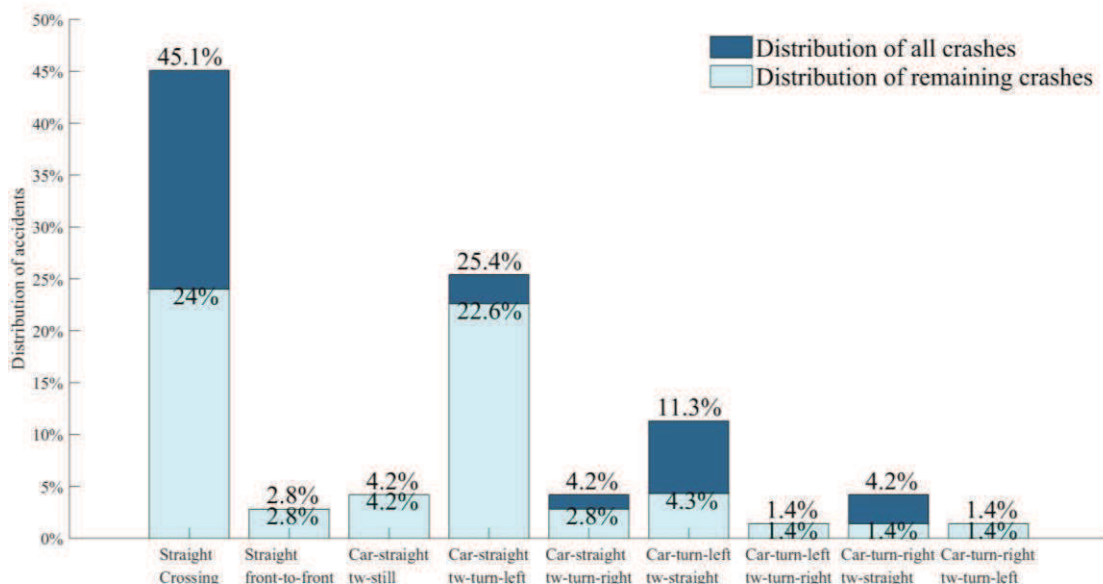

Figure 3.4   Distribution of the remaining crashes after AEB implementation, compared to the original number (all) crashes. The proportion of the remaining crashes is calculated by dividing the remaining crash numbers by the total number of crashes in the original, where

the dark blue (based on original crashes) sums up to 100%, while to sum of the light blue shows the percent remaining crashes, approximately 65%.

As shown in Table 3.3, the proportions of different scenario types are compared between the original crashes and the remaining crashes.

Table 3.3   Comparison of scenario type proportions between original crashes and remaining crashes

Scenario Type	Original crashes	Remaining crashes
Straight crossing	45.1%	36.9%
Straight front-to-front	2.8%	4.3%
Car straight, two-wheeler still	4.2%	6.5%
Car straight, two-wheeler turns left	25.4%	34.8%
Car straight, two-wheeler turns right	4.2%	4.3%
Car turns left, two-wheeler straight	11.3%	6.6%
Car turns left, two-wheeler turns right	1.4%	2.2%
Car turns right, two-wheeler straight	4.2%	2.2%
Car turns right, two-wheeler turns left	1.4%	2.2%
Total	100%	100%

For the proposed algorithm, the effectiveness is approximately 35% of all scenarios (see, 3.1, AEB algorithm simulation results). Figure 3.5 presents the effectiveness of the proposed algorithm for each single scenario. It shows that the three scenarios, 'Straight crossing', 'Car turning left, two-wheeler straight' and 'car turning right and two-wheeler straight', have better effectiveness than the average effectiveness result. The top two scenarios are both car turning cases, including the 'Car turning left, two-wheeler straight' scenario with the AEB effectiveness of 64% and the 'car turning right and two-wheeler straight' scenario with 75%. The remaining car turning cases are the 'car turning left, two-wheeler turning right' scenario and the 'car turning right, two-wheeler turning left' scenario. As shown in Figure 3.4, these two types of scenarios only take 1% of the total 71 cases respectively.
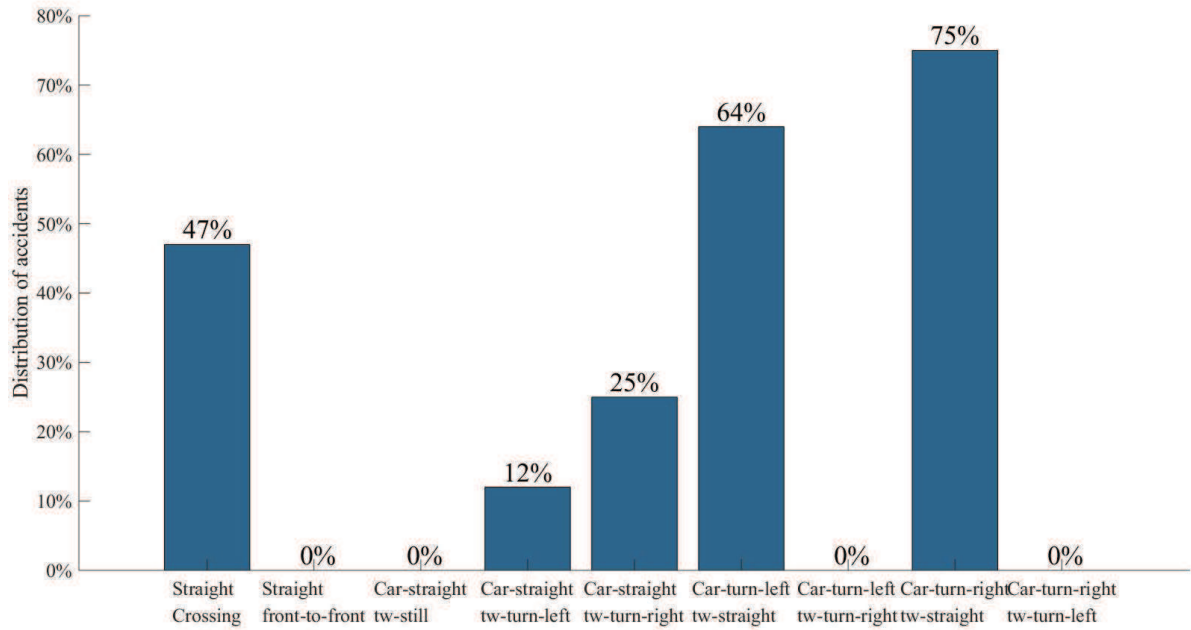
Figure 3.5   Effectiveness distribution of the AEB for each scenario, calculated by dividing the number of avoided crashes by the number of crashes of the same type scenario.

After all the car tuning or car straight moving cases were grouped together, the AEB effectiveness were calculated for these two types of cases. As shown in Figure 3.6, the effectiveness of the AEB for turning car type is much higher than that of the straight moving car type.

Figure 3.6   Avoidance results for straight and turning car

3.2.2 Speed reduction

Figure 3.7 shows the changes of the impact speed for the remaining crashes after the AEB implementation. It shows that for all the cases, the new impact speed is lower than the original impact speed.
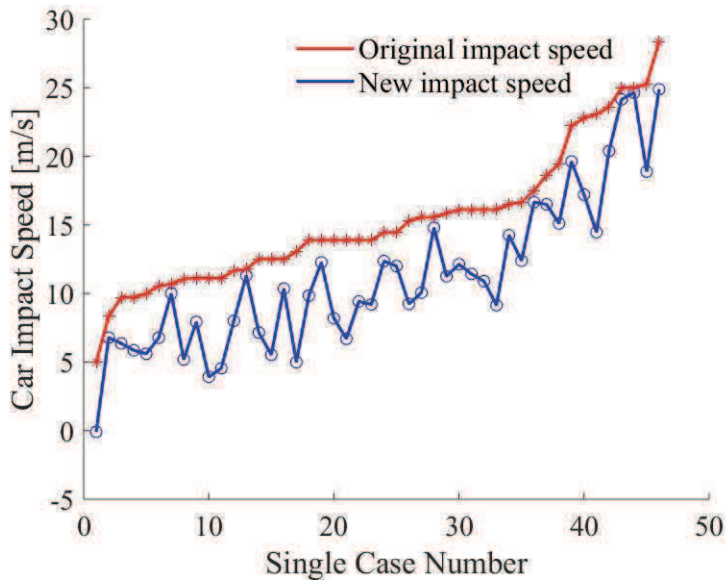
Figure 3.7   Comparison between the car's original impact speed and the new impact speed after the AEB implementation. The cases have been sorted by the original impact speed

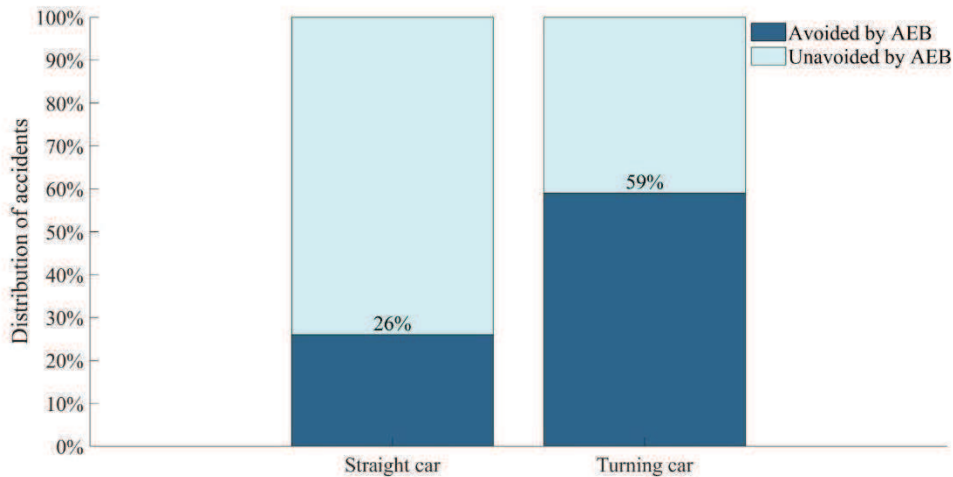The reduction of the speed and its distribution for all the remaining cases are shown in Figure 3.8. It indicates that the maximum speed reduction is within 10m/s. The plot of the speed reduction and the original impact speed does not indicate a specific relation between them. The speed reduction distribution plot shows that the most speed reduction is between 3m/s and 6m/s.
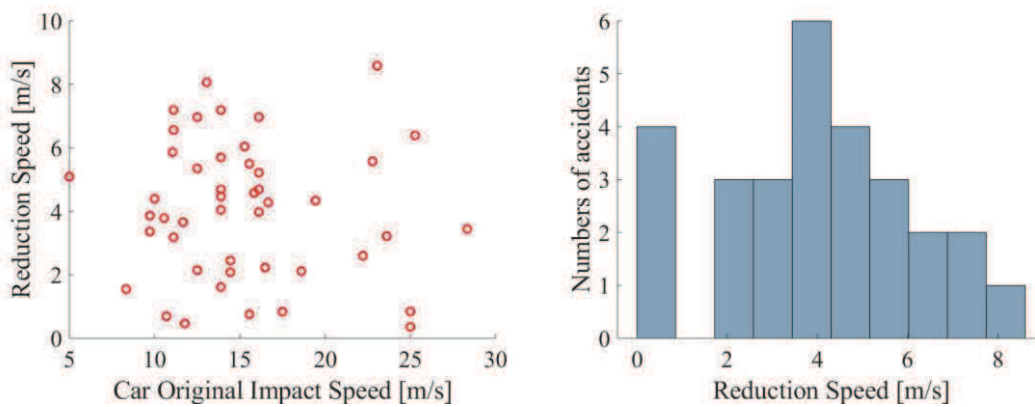
Figure 3.8   Reduced speed and original impact speed of car. And distribution of reduced speed of car.

3.2.3 Speed characteristics

Figure 3.9 shows the speed distribution of the car and the two-wheeler regarding avoided and unavoided cases. This plot clearly suggests the difference of the speed characteristics for the unavoided cases from the avoided cases. For the unavoided cases, the speeds of the two-wheeler are not high, almost under 10m/s, and the speed of the car are relatively high, mostly greater than 10m/s.
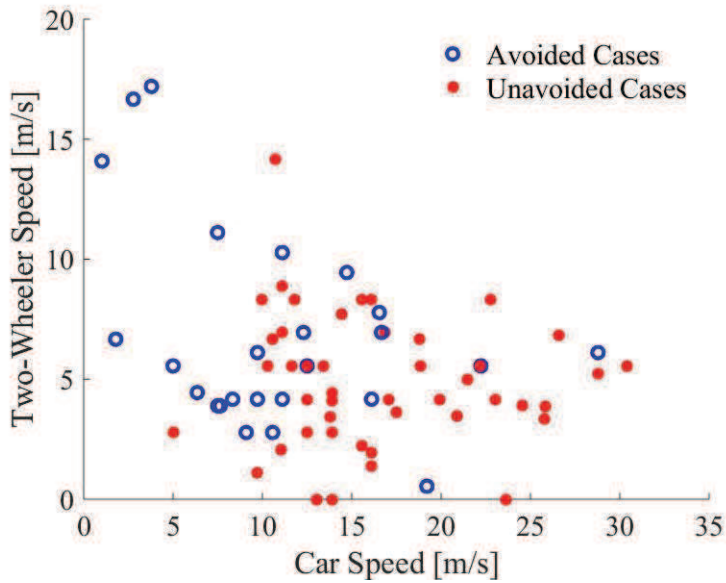
Figure 3.9   Scatter plot of the speed of the car and the two-wheeler when the AEB system activates. The blue hollow circles are the avoided cases and red solid dots are the unavoided cases.

The speed distribution plot also shows the same remaining crashes speed characteristics, and is shown in Figure 3.10. For the cases not avoided by AEB, most of them occur with a relatively high car speed. On the contrary, the crashes avoided mainly occur with lower car speed than the unavoided crashes.
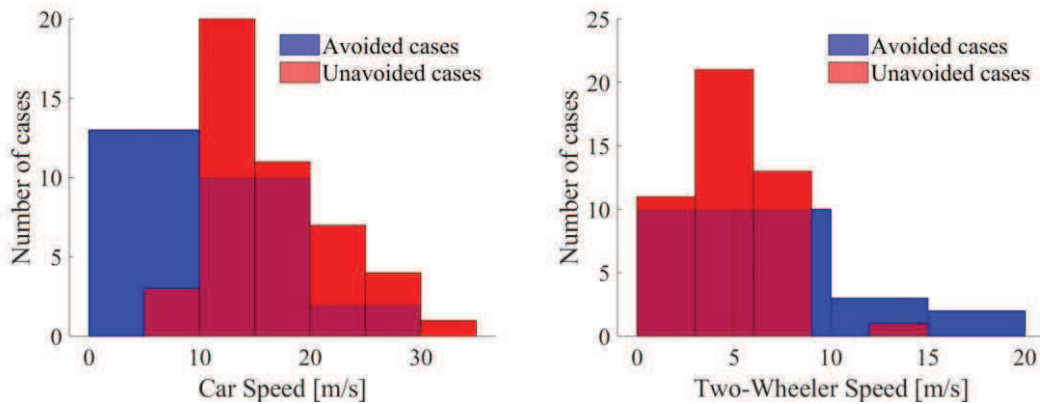
Figure 3.10   Speed distribution of the avoided and the unavoided cases for both the car and the two-wheeler.

3.2.4 Residual injury analysis

Figure 3.11 shows the changes of impact speed after the AEB implementation for the remaining crashes. For each single case, the new relative impact speed is smaller than the original relative impact speed.
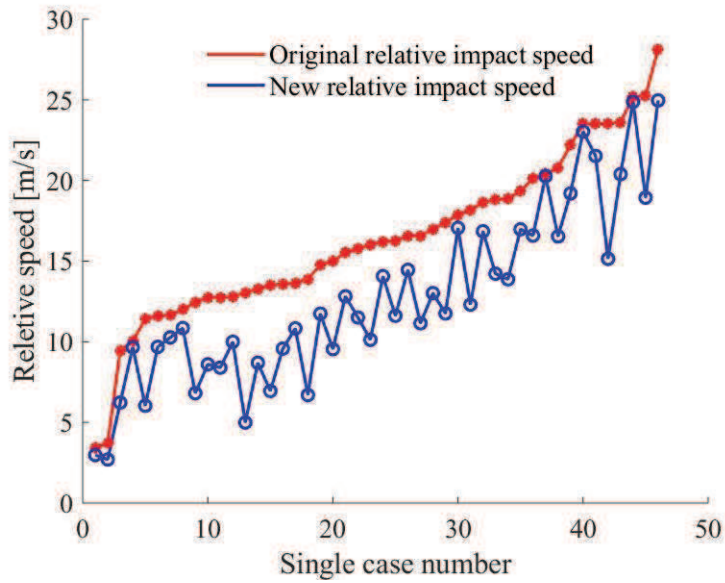
Figure 3.11 Comparison between the original relative impact speed and the new relative impact speed of the car after the AEB implementation.

Table 3.4 shows the effectiveness of different injury risk reduction regarding the remaining crashes. It indicates that the reduction effectiveness of MAIS2+F and MAIS3+F injury are approximately 30% and approximately 40% for the fatal injuries.

Table 3.4   Mean effectiveness of different injury levels regarding the remaining crashes

Injury level	MAIS2+F	MAIS3+F	fatal
Mean effectiveness	29.87%	31.21%	40.09%

4 Discussion

This study presents an AEB algorithm for cars in car-to-two-wheeler crashes, based on comfort limits of car drivers and two-wheeler drivers and the braking capabilities of the cars. The algorithm has been applied to the SHUFO PCM in virtual simulations, to evaluate the performance of the AEB. The simulation results of the proposed algorithm were compared with a reference AEB algorithm which is based on the braking limit of the vehicle. These results indicated that AEB would have a beneficial traffic safety influence by avoiding or mitigating a large proportion of car-to-two-wheeler crashes in China. However, taking the car and two-wheeler drivers' comfort limits into account, aiming to minimize nuisance AEB interventions, reduce the effectiveness of the system by more than a factor of two, compared to the reference algorithm that only considers limitations of the car itself. The effectiveness in collision avoidance varies across scenarios, and the proposed algorithm shows more potential in car turning scenarios.

Based on the comparison of trigger time results, for approximately 50% cases, the proposed AEB algorithm is triggered closer to collision than the reference AEB algorithm. It indicates that if the AEB system is triggered according to the reference AEB algorithm, half of the drivers still have time to avoid collision on their own or by actions of the two-wheeler drivers, still not having crossed their comfort zone boundaries. This suggests unnecessary AEB interventions for the half of the crashes if the reference algorithm would be used. These situations may be considered nuisance AEB interventions for a driver, as he/she may have been able to comfortably avoid the crash also after the (reference algorithm) AEB intervened. Also, based on the results of the TTC time, the proposed AEB algorithm has smaller TTC than the reference algorithm when the AEB intervenes and it suggests that the proposed AEB algorithm intervenes later than the reference AEB algorithm when the situation is more severe. As the effectiveness of the proposed AEB algorithm is lower than the reference AEB algorithm, more crashes are unavoidable by the proposed AEB algorithm than the reference AEB algorithm, but the system would also be more acceptable by drivers. Regarding the brake intervention, as a car would stop earlier if the crash is not avoided, so the brake duration can be shorter for the case whose crash is not avoided. Therefore, as the proposed AEB algorithm has more unavoidable crashes, the brake durations are shorter than that of the reference AEB algorithm, as shown in Figure 3.3.

The two algorithms were compared with respect to their effectiveness in collision avoidance. The effectiveness of the proposed AEB algorithm is approximately 35%, while the effectiveness of the reference algorithm is 71%. The relatively low effectiveness of the proposed algorithm for this dataset is due to the fact that it considers four maneuvers of both drivers and the AEB is triggered only when the drivers cannot avoid collision by steering or braking comfortably (with a comfortable limit of $5m/s^2$ longitudinally and $5m/s^2$ laterally, see 2.3.3 Braking maneuver and 2.3.4 Steering maneuver). However, the original crash data contains actual crashes and drivers from the dataset did not avoid the crashes. So, when the proposed AEB system is triggered, it can be too late to avoid the crash regarding the crash dataset (but often with impact speed reductions, see Figure 3.8, still making the system beneficial). Among the crash cases not avoidable by the AEB, a large number of them could possibly be avoided by the car driver steering, or the two-wheeler driver braking or steering, or the Automatic Emergency Steering (AES) system for the car or the two-wheeler. In reality, the drivers could have the chance to brake or steer in time to avoid the crash, and the

AES system would likely be beneficial in collision avoidance also after the drivers have passed their comfort limits of steering.

The effectiveness of AEB also varies across scenarios. The effectiveness of the turning car scenario is 59% and of the straight moving car scenario is 26%. This result are in line with results from the study of another researcher who also indicated that the AEB intervention is more effective for the turning vehicle scenarios than for the straight moving vehicle scenarios (Sander, 2017).

The original crash data was classified into nine types of scenarios based on the course direction, heading angle and velocities of cars and two-wheelers. The largest three scenario groups are: 'straight crossing', 'car straight and two-wheeler turning left', and 'car turning left and two-wheeler going straight' for both the original crashes and the remaining crashes (after the proposed AEB algorithm is applied to the original crash data). However, the proportion of different scenario types varies between the original crashes and the remaining crashes. The straight crossing type accounts for 45.1% of all crashes for the original crashes, while 36.9% for the remaining cases (see, Table 3.3). For the car straight and two-wheeler turning left type scenario, it has a proportion of 25.4% of all crashes for the original crashes, and 34.8% for the remaining cases with a 9.4% increase (see, Table 3.3). The car turning left and two-wheeler going straight type scenario accounts for 11.3% of all crashes for the original crashes, and is decreased to 6.6% for the remaining cases (see, Table 3.3). Even though the straight crossing type has a smaller proportion in remaining crashes than in original crashes, the other two car and two-wheeler straight going types (straight front-to-front type, and car straight, two-wheeler still type) instead account for a larger part in remaining crashes and the sum of these three straight types has only an increase of 4.4% in the remaining crashes. The other six scenario types have few cases and does not change much in terms of proportion of original crashes and remaining crashes.

Based on the comparison of the original impact speed and new impact speed after the AEB implementation, a specific relationship between the reduced speed and the original speed cannot be concluded. However, studying the characteristics of the unavoided crashes, the trigger speed scatter plot indicates that most unavoidable cases take place when the car speed is relatively high, typically above 10m/s, and when the two-wheeler speed is below 10m/s. According to the 'brake or steer strategy' in another study (Brännström et al., 2014), using a steering maneuver is a better strategy than braking when the car speed is high. However, an AEB system only has braking reaction. Consequently, when the car speed is high, AEB effectiveness is low. Therefore, most unavoidable crashes involve a car travelling at high speed.

The results related to injury reduction suggest the proposed AEB algorithm has a beneficial influence in injury reduction. For total crashes, the reduction effectiveness for fatal injury is around 60% and for MAIS2+F and MAIS3+F, around 50%.

Two types of steering were studied in previous research (Sander, 2017, 2018) and steering styles were taken into account in this study. 'J-steering type', where the steering wheel angle is increased with constant steering wheel angle rate, is implemented in this algorithm. Other researchers have investigated more complex 'S-steering type' steering strategy, with a sinusoidal steering input for a predefined offset (Sander, 2017, 2018). With the S-steering, the car heads towards the same direction before and after the steering maneuver, while the

car just steers away with the J-steering. As the algorithm is applied to all types of scenarios, different types of situations increase the complexity for implementing s-steering, therefore, only J-steering was adopted in this study (due to time constraints).

Some errors in the data were also found during the implementation of the algorithm. For ten cases, the maximum acceleration from the vehicle dynamics data was beyond the maximum acceleration based on the road friction coefficient. For the reference algorithm, the braking limitation of the vehicle is the input parameter. This error is taken into consideration when the reference algorithm is designed. Instead of using the road friction coefficient as the reference AEB braking level, the larger value of the road friction multiplied gravity acceleration and the maximum braking acceleration from the original data was adopted. It ensured the reference AEB braking level is the maximum braking level of the vehicle for the dataset. Another data error is that the lateral acceleration is above 20 m/s^2 for six cases. From other literature study, the maximum lateral acceleration of vehicle was assumed to be 7 m/s^2 (Brännström et al., 2008). Accelerations higher than 10 m/s^2 is not physically possible only due to simple friction, but irregularities in the contact surfaces, gripping or hitting objects can make it reach a little bit higher than 10 m/s^2, but 20 m/s^2 on a normal roadway is very unlikely. For the braking maneuvers inside the proposed algorithm, the acceleration value at each timestep was utilized. This type of error could have influenced the results of the AEB algorithm. The proposed algorithm has been modified to avoid this bias influence. In the modified codes, the acceleration value was only considered when it is within 20 m/s^2. Otherwise, the acceleration value was not used in the simulations and the braking acceleration is assumed to start from zero. Therefore, the erroneous wrong lateral acceleration problem is addressed.

The study considers possible braking and steering maneuvers of car drivers and two-wheeler drivers. However, each maneuver is independent from the others and the algorithm only considers the situation where only one maneuver happens at a time. Even though two or three maneuvers could possibly occur at the same time, the probabilities are low. In this study, the combination of different maneuvers is not included.

4.1 Limitation

One limitation is the limited number of car-to-two-wheeler cases (71) used in this study. Also, the pre-crash time of some cases is very short, for example, 16 cases have PCM of less than two seconds. When the time series are short, the crash cannot be avoided even if the AEB algorithm applies in the beginning of the time series, which can influence the effectiveness results.

The data was derived from reconstruction, not from recordings of the crashes directly, and the quality and accuracy of reconstruction information is difficult to assess. As discussed in this chapter (see, 4, Discussion), some errors were detected in the data, therefore, the data cannot be expected to be entirely accurate also elsewhere. All 71 cases were divided into nine scenario types and some scenario types have very limited number of cases. For example, six scenario types respectively take up less than 5% of the whole set of accidents. Therefore, when the effectiveness of the AEB for each scenario is evaluated, these scenario types are too few to be good references for study.

The analysis related to the motorcyclist injury is based on the available motorcyclist injury model, not on a systematic review of risk curves as no other injury curves are available. The reference paper is a recent publication and not a review paper, and the quality of the paper is not discussed in this work. Actually, the risk curves were taken from literature as the only clear mathematical relation between impact condition and injury outcome. As there are no review papers and meta-analyses available, the quality and generalizability is hard to assess. The use of relative speed does not necessarily correlate with the energy brought into the impact. Other impact severity measures such as delta velocity or impact speed have been used in risk curves for car occupants or pedestrians, but application to motorcyclists that have substantial own speed and can separate from the motorcycle is not obvious. The authors of the used risk curves (Ding et al., 2019) claims relative velocity gives high prediction accuracy and is a useful measure. Fatality risk at high relative speeds is substantially lower than most studies found for pedestrians (Hussain, Feng, Grzebieta, Brijs, & Olivier, 2019). As noted in (Rosén, 2013), this might be due to impacts to the motorcycle instead of the rider, while pedestrian impacts are always to the pedestrian. However, it was beyond of the scope if the thesis to thoroughly evaluate and potentially construct other risk curves.

The one-track bicycle model is used in this study, however, this vehicle model is not realistic for cars. In the simulations, however, this vehicle model is only relevant for the calculation of avoidance by comfortable steering, not for avoidance by comfortable braking.

The generalizability of the crash data was in Jiading distinct in Shanghai. Jiading is a rural area, therefore, the data used in this study is representative for rural area. The sensor models are part of the simulation framework, and in the simulations, no sensor issues or issues with tracking data is included. The sensors are assumed to work perfectly without any error, which is not realistic in real applications.

4.2 Future research direction

The three following areas can be useful for further research.

A natural next study would include AEB performance when different combinations of braking comfort limits of car drivers and two-wheeler drivers are applied. Especially for the two-wheeler drivers, as the available study of braking level is limited, it is necessary to study the AEB results based on different braking limitations of two-wheeler drivers.

While the current research is about single maneuver, another future research direction is to combine different maneuvers together. For example, car driver steering maneuver and two-wheeler driver braking maneuver happen at the same time. To make it more practical, a probability framework of different single maneuvers and multi maneuvers can be built by considering the possibility of using a single maneuver or combined maneuvers. In addition, the s-shape steering maneuver may be compared with the j-shape, to evaluate the effect of the different types of steering maneuver profiles.

In this study, the AEB intervention is only applied to the car but not the two-wheeler. As the AEB system is also available for two-wheelers on the market, study of the residual crashes after the implementation of the AEB algorithms to the two-wheeler can be interesting as well.

The simulation framework in this study can also be applied to other PCM databases for further study.

5 Conclusion

In this study, an AEB algorithm based on drivers possible maneuvers to avoid collision is proposed. Trajectory prediction, braking and steering maneuvers are included in the algorithm. This algorithm is computed for each timestep and is applicable to all types of car-to-two-wheeler crash scenarios. After implementing the algorithm to car-to-two-wheeler crashes in China, the results indicate that this algorithm can avoid approximately 35% of car-to-two-wheeler crashes by using the specific driver comfort limits. This is less than half the effectiveness of the reference algorithm, which disregards drivers acceptance and potential nuisance AEB interventions. The injury risk of two-wheelers can be mitigated ranging between 50% to 60% for three injury levels including MAIS2+F, MAIS3+F and fatalities. This algorithm also implies different crash avoidance functionality in different scenarios. It was found that the AEB intervention for the car turning scenarios is more effective than in straight moving car scenarios, in line with previous research. Furthermore, AEB intervention shows relatively low effectiveness when car speed is high, as the car has more potential to steer than brake to avoid collision at high speed.

This study can help designers of active safety systems and automated vehicles, as well as designers of injury prevention measures, as it provides an AEB algorithm aiming minimum nuisance for drivers and describes the remaining crash characteristics after the AEB implementation. The proposed AEB algorithm, which shows potential in crash avoidance and mitigation, can help further development of crash avoidance system, and the simulation results present the remaining injuries which could not be avoided by the proposed active safety system and needs further injury prevention methods.

6 Reference

Abe, M., & Manning, W. (2009). Fundamentals of Vehicle Dynamics. In *Vehicle Handling Dynamics*. https://doi.org/10.1016/b978-1-85617-749-8.00003-9

Bärgman, J., Smith, K., & Werneke, J. (2015). Quantifying drivers' comfort-zone and dread-zone boundaries in left turn across path/opposite direction (LTAP/OD) scenarios. *Transportation Research Part F: Traffic Psychology and Behaviour*. https://doi.org/10.1016/j.trf.2015.10.003

Bartolomeos, K., Elkington, J., Harvey, A., Ivers, R., Khayesi, M., Peden, M., … Organization, W. H. (2017). *Powered Two- and Three-Wheeler Safety: A Road Safety Manual for Decision-Makers and Practitioners*. 108p. Retrieved from http://apps.who.int/iris/bitstream/10665/254759/1/9789241511926-eng.pdf%0Ahttps://trid.trb.org/view/1466127

Brännström, M., Coelingh, E., & Sjöberg, J. (2010). Model-based threat assessment for avoiding arbitrary vehicle collisions. *IEEE Transactions on Intelligent Transportation Systems*. https://doi.org/10.1109/TITS.2010.2048314

Brännström, M., Coelingh, E., & Sjöberg, J. (2013). Decision-making on when to brake and when to steer to avoid a collision. *International Journal of Vehicle Safety*, 7(1), 87. https://doi.org/10.1504/ijvs.2014.058243

Brännström, M., Coelingh, E., & Sjöerg, J. (2009). Threat assessment for avoiding collisions with turning vehicles. *IEEE Intelligent Vehicles Symposium, Proceedings*. https://doi.org/10.1109/IVS.2009.5164356

Brännström, M., Sjöberg, J., & Coelingh, E. (2008). A situation and threat assessment algorithm for a rear-end collision avoidance system. *IEEE Intelligent Vehicles Symposium, Proceedings*, 102–107. https://doi.org/10.1109/IVS.2008.4621250

China Automotive Technology and Research Center. (2018). *C-NCAP Management Regulation*.

Coelingh, E., Eidehall, A., & Bengtsson, M. (2010). Collision warning with full auto brake and pedestrian detection - A practical example of automatic emergency braking. *IEEE Conference on Intelligent Transportation Systems, Proceedings, ITSC*. https://doi.org/10.1109/ITSC.2010.5625077

Coelingh, E., Jakobsson, L., Lind, H., & Lindman, M. (2007). Collision Warning With Auto Brake - a Real-Life Safety Perspective. *Proceedings of the 19th International Conference on Enhanced Safety of Vehicles (ESV)*, (June 2015), 1–9.

Coelingh, E., Lind, H., Birk, W., & Wetterberg, D. (2006). Collision warning with auto brake. *FISTA World Congress*.

Costa, L., Perrin, C., Dubois-lounis, M., Serre, T., Costa, L., Perrin, C., … Nacer, M. (2019). *Modeling of the Powered Two-Wheeler dynamic behavior for emergency situations analysis To cite this version : HAL Id : hal-02078039*.

Dahl, J., de Campos, G. R., Olsson, C., & Fredriksson, J. (2018). Collision Avoidance: A Literature Review on Threat-Assessment Techniques. *IEEE Transactions on Intelligent Vehicles*. https://doi.org/10.1109/tiv.2018.2886682

Ding, C., Bohman, K., Zhang, W., Li, Y., & Zhao, X. (2016). Rear seated occupants in near-side impacts -study based on Chinese accident databases. *13th International Forum of Automotive Traffic Safety (INFATS)*, 0–5.

Ding, C., Rizzi, M., Strandroth, J., Sander, U., & Lubbe, N. (2019). Motorcyclist injury risk as a function of real-life crash speed and other contributing factors. *Accident Analysis and Prevention*. https://doi.org/10.1016/j.aap.2018.12.010

Euro NCAP. (2018). *EUROPEAN NEW CAR ASSESSMENT PROGRAMME (Euro NCAP) ASSESSMENT PROTOCOL – SAFETY ASSIST*. (November).

European Commission. (2015). *Traffic Basic Facts 2015 Motorcycles and Mopeds*.

Genève, & Bastiaensen, E. (2014). *The Shared Road to Safety A Global Approach for Safer Motorcycling*. (May).

Gennarelli, T. A., & Wodzin, E. (2006). AIS 2005: A contemporary injury scale. *Injury*. https://doi.org/10.1016/j.injury.2006.07.009

Godthelp, H. (1986). Vehicle control during curve driving. *Human Factors*. https://doi.org/10.1177/001872088602800209

Horst, R. Van Der, Hogema, J., Van Der Horst, R., Hogema, J., Horst, R. Van Der, & Hogema, J. (1993). Time-to-collision and collision avoidance systems. *Proceedings of The 6th ICTCT Workshop*.

Jeppsson, H., Östling, M., & Lubbe, N. (2018). Real life safety benefits of increasing brake deceleration in car-to-pedestrian accidents: Simulation of Vacuum Emergency Braking. *Accident Analysis and Prevention*, *111*(December 2017), 311–320. https://doi.org/10.1016/j.aap.2017.12.001

Jiang, L., He, J., Liu, W., & Zhu, X. (2014). Research on Test Scenarios of Automatic Emergency Braking System. *Automobile Technology*, *1*, 39–43.

Li, Y., Qiu, J., Liu, G. D., Zhou, J. H., Zhang, L., Wang, Z. G., … Jiang, Z. Q. (2008). Motorcycle accidents in China. *Chinese Journal of Traumatology - English Edition*. https://doi.org/10.1016/S1008-1275(08)60050-4

New South Wales Government. (2012). *NSW Motorcycle Safety Strategy*.

NHTSA. (2018). *Traffic safety facts 2016 (DOT HS 812 554)*. (February).

O'Neill, B. (2009). Preventing passenger vehicle occupant injuries by vehicle Design- A historical perspective from IIHS. *Traffic Injury Prevention*. https://doi.org/10.1080/15389580802486225

OICA. (2018). *World Vehicles in Use (By Country and Type 2005-2015)*. *2015*, 2. Retrieved from http://www.oica.net/wp-content/uploads//Total_in-use-All-Vehicles.pdf

Road Safety Authority. (2014). *National Motorcycle Safety Action Plan 2010-2014*.

Rosén, E. (2013). Autonomous Emergency Braking for Vulnerable Road Users. *Proceedings of the 2013 International IRCOBI Conference on the Biomechanics of Injury*, 618–627.

Sander, U. (2017). Opportunities and limitations for intersection collision intervention—A study of real world 'left turn across path' accidents. *Accident Analysis and Prevention*. https://doi.org/10.1016/j.aap.2016.12.011

Sander, U. (2018). *Predicting Safety Benefits of Automated Emergency Braking at Intersections Virtual simulations based on real-world accident data*.

Schubert, A., Erbsmehl, C., & Hannawald, L. (2013). Standardized pre-crash scenarios in digital format on the basis of the VUFO simulation input data from GIDAS. *5th International Conference on ESAR „Expert Symposium on Accident Research"*.

Sui, B., Zhou, S., & Lubbe, N. (n.d.). *Real world analysis of in-car child occupant safety in China*. 1–10.

Tageldin, A., Sayed, T., & Wang, X. (2016). Can Time Proximity Measures Be Used as Safety Indicators in All Driving Cultures? *Transportation Research Record: Journal of the Transportation Research Board*. https://doi.org/10.3141/2520-19

Uittenbogaard, J., Op den Camp, O., & van Montfort, S. (2016). *CATS Deliverable 2.2: CATS car-to-cyclist accident parameters and test scenarios*. Retrieved from www.TNO.nl/CATS

World Health Organization. (2018). Global status report on road safety 2018. In *WHO*.